AIAA JOURNAL
Vol. 46, No. 5, May 2008

Improved Component-Mode Synthesis for Nonclassically Damped Systems

M. H. Liu*
Harbin Institute of Technology, 150001 Harbin, People's Republic of China
and
G. T. Zheng†
Tsinghua University, 100084 Beijing, People's Republic of China

DOI: 10.2514/1.32869

An improved technique of the component-mode synthesis for nonclassically damped systems with the second-order approximation is proposed in this paper. It is based on free-interface vibration modes and residual attachment modes or residual inertia-relief attachment modes complemented with dynamic effects of the truncated modes. Both nondefective and defective components are considered, and the relationships between them are discussed. A new criterion for the selection of the component vibration modes is developed in the frequency domain. State-level synthesis procedures are naturally employed in the new formulations presented herein. The accuracy and effectiveness of the present synthesis method are demonstrated and are compared with those of the static approach via numerical examples, and also the validity of the modes selection criterion is also proved by these examples.

Nomenclature

A_s, B_s	=	synthesized system matrices
C	=	damping matrix of the component
f	=	external force vector acting on the component
I	=	identity matrix
K	=	stiffness matrix of the component
M	=	mass matrix of the component
p	=	modal coordinate vector
T	=	transformation matrix between independent and dependent modal coordinates
x	=	unknown displacement response vector of the component
λ_i	=	complex eigenvalue of the component
Λ	=	complex spectrum matrix
φ_i, ψ_i	=	right and left eigenvectors of the component in the state space
Φ, Ψ	=	right and left modal matrices in the state space
$\bar{\Phi}$	=	component mode used for the synthesis
Φ^d_{rd}, Ψ^d_{rd}	=	right and left rigid-body modes in the displacement space

Subscripts

a	=	set of residual attachment modes
e	=	set of elastic complex modes
ek	=	set of kept elastic complex modes
k	=	set of kept complex modes
r	=	set of rigid-body modes
t	=	set of truncated complex modes

Superscripts

α	=	component α
β	=	component β

Received 17 June 2007; revision received 17 December 2007; accepted for publication 30 December 2007. Copyright © 2008 by the American Institute of Aeronautics and Astronautics, Inc. All rights reserved. Copies of this paper may be made for personal or internal use, on condition that the copier pay the $10.00 per-copy fee to the Copyright Clearance Center, Inc., 222 Rosewood Drive, Danvers, MA 01923; include the code 0001-1452/08 $10.00 in correspondence with the CCC.

*Ph.D. Student, Department of Astronautics and Applied Mechanics, P.O. Box 137; mhliu.hit.edu.cn@gmail.com.

†Professor, Department of Astronautics and Aeronautics, P.O. Box 20; gtzhengtu@yahoo.co.uk.

I. Introduction

COMPONENT-MODE-SYNTHESIS (CMS) methods are usually employed to provide reduced-order models with required model accuracy for further analyses or to predict dynamic responses of large models via a reduced-size problem. CMS techniques for undamped or proportional damped systems have been well developed over the past four decades [1–8]. However, modern structures are often heavily damped due to extensive applications of composite materials and/or various energy dissipation techniques, and hence the simplification of undamped systems and the hypothesis of proportional damping are not appropriate anymore in many cases. As a consequence, conventional CMS techniques developed before may not provide results of the required accuracy or correctness for such structures. Nevertheless, few works have been done for the application of CMS to nonclassically damped systems.

Howsman and Craig [9] developed a state-space free-interface synthesis procedure that employs a set of free-interface vibration modes along with a set of attachment modes. Beliveau and Soucy [10] developed a modified Craig–Bampton method by replacing the real fixed-interface normal modes with the corresponding complex modes. Craig and Ni [11] generalized the concepts of residual flexibility and residual attachment modes to damped systems and then presented a state-space free-interface component-mode-synthesis method that achieves greater model accuracies than those by the previous methods. Their approach was later extended to the analysis of damped multicomponent systems with both flexible and rigid interfaces and was compared with real CMS for various levels of damping and mode truncations [12]. In [13] the authors used the method of weak springs to treat unconstrained components and made a selection procedure of retained modes based on the absolute values of the complex eigenvalues. A distinctive fixed-interface CMS method was shown in the subspace spanned by real Schur vectors rather than complex eigenvectors [14]. The newly proposed constraint modes CMS method by Morgan et al. [15] is another extension of the Craig–Bampton method in the state space. And other studies on the subject of the component-mode synthesis for damped systems can be found in [16–22].

This paper presents an improved technique of the component-mode synthesis for nonclassically damped systems in the state space for the purpose of model order reduction. The proposed method is based on the concepts of residual flexibility and residual attachment modes as described by Craig and Ni [11], but the so-called

second-order approximations are developed and are used to improve the accuracy and effectiveness of the synthesis procedure. The second-order approximations are developed for both nondefective and defective components; however, different approaches are used in the development procedures. A specific criterion for the selection of retained component modes is established by means of the error analysis of the frequency response function (FRF). The formulations are first demonstrated on a nonclassically damped free–free beam model and then further examined on a satellite structure.

II. Dynamic Equations in State-Space Form

The equation of motion for a linear dynamic system can be written in a standard form as a matrix ordinary differential equation:

$$M\ddot{x}(t) + C\dot{x}(t) + Kx(t) = f(t) \tag{1}$$

where M, C, and K are real and constant and the only assumption on them is that M is positive-definite.

When the damping matrix C cannot be diagonalized simultaneously with M and K by real normal modes, the system is considered as nonclassically damped. To decouple the dynamic equation, the double-sized state-space form of Eq. (1) is often used, which is

$$A\dot{y} + By = F \tag{2}$$

where

$$A = \begin{pmatrix} C & M \\ M & O \end{pmatrix} \qquad B = \begin{pmatrix} K & O \\ O & -M \end{pmatrix} \tag{3}$$

and

$$y = \begin{pmatrix} x \\ \dot{x} \end{pmatrix} \qquad F = \begin{pmatrix} f \\ 0 \end{pmatrix} \tag{4}$$

are referred to as the state mass matrix, the state stiffness matrix, the state response vector, and the state load vector, respectively.

The right state-space eigenproblem is obtained by assuming $y = \varphi e^{\lambda t}$ for the free vibration of Eq. (2):

$$(\lambda_i A + B)\varphi_i = 0 \qquad i = 1, 2, \ldots, 2n \tag{5}$$

where the eigenvalue λ_i and eigenvector φ_i are complex and in conjugate pairs for underdamped modes, and there may also be an even number of real eigenvalues and eigenvectors for overdamped modes; n is the number of degrees of freedom (DOF) of the system.

The left or adjoint state-space eigenproblem for Eq. (5) can be written as

$$(\lambda_i A^T + B^T)\psi_i = 0 \qquad i = 1, 2, \ldots, 2n \tag{6}$$

It plays a significant role in the biorthogonality and complex modal analysis theories. If M, C, and K are all symmetric, the system is self-adjoint, and Eq. (6) is not needed.

For forced response calculation, the state response vector can be expressed as

$$y = \sum_{i=1}^{2n} \varphi_i p_i \tag{7}$$

where p_i is the modal coordinate that can be solved from a set of decoupled (for the nondefective eigensystem, as will be described later) complex modal equations.

The exact solution of y can be approximated by

$$y \approx \begin{pmatrix} \Phi_k & \Phi_a \end{pmatrix} \begin{pmatrix} p_k \\ p_a \end{pmatrix} \tag{8}$$

where Φ_k is the kept complex modal matrix composed of a much smaller number of important system modes, and Φ_a has as many columns as the excitation DOF and is defined as the state-space residual attachment modes, which are an approximation to the truncated modes. The importance of the vibration modes will be ranked by a specific criterion developed later.

III. Improved Residual Attachment Modes

In CMS procedures, all equations in the preceding section can be applied to nonclassically damped components with a free interface, and the load vector $f(t)$ will contain interface forces and external forces. When the free-interface CMS is used, it is found convenient to classify components as nondefective and defective for improving residual attachment modes.

A. Nondefective Components

If the component has no rigid-body modes and any of the nonzero eigenvalues of its eigensystem hold the same geometric and algebraic multiplicity, the eigensystem is said to be nondefective, as is the component. Obviously, components being constrained and without repeated eigenvalues are nondefective.

For nondefective components, the fully decoupled complex modal equations of motion are obtained by substituting transformation $y = \Phi p$ [i.e., Eq. (7)] into Eq. (2) and premultiplying it by Ψ^T:

$$\begin{pmatrix} \dot{p}_k \\ \dot{p}_t \end{pmatrix} - \begin{pmatrix} \Lambda_k & 0 \\ 0 & \Lambda_t \end{pmatrix} \begin{pmatrix} p_k \\ p_t \end{pmatrix} = \begin{pmatrix} \Psi_k^T \\ \Psi_t^T \end{pmatrix} F \tag{9}$$

where the right eigenvector matrix $\Phi = (\varphi_1 \quad \varphi_2 \quad \cdots \quad \varphi_{2n})$ is partitioned into two sets, kept modes Φ_k and truncated modes Φ_t and, consequently, the partitioned left eigenvector matrix $\Psi = (\psi_1 \quad \psi_2 \quad \cdots \quad \psi_{2n})$ and complex spectrum matrix $\Lambda = \text{diag}\{\lambda_1 \quad \lambda_2 \quad \cdots \quad \lambda_{2n}\}$.

Note that the biorthogonality and A-normalization of Φ and Ψ are used in Eq. (9) for decoupling modal coordinates, which are

$$\Psi^T A \Phi = I \qquad \Psi^T B \Phi = -\Lambda \tag{10}$$

For harmonic loads with frequency ω, the complex response $\dot{p} = j\omega p$ ($j = \sqrt{-1}$) exists. So with the Neumann-series expansion, the truncated modal coordinates p_t can be obtained from the second set of Eq. (9):

$$\begin{aligned} p_t &= (j\omega I - \Lambda_t)^{-1} \Psi_t^T F \\ &= -\Lambda_t^{-1}[I + j\omega\Lambda_t^{-1} + (j\omega\Lambda_t^{-1})^2 + \cdots]\Psi_t^T F \end{aligned} \tag{11}$$

where the infinite series in the bracket converges if and only if $|j\omega| < \min(|\Lambda_t|)$.

If only the first term of the infinite series appearing in Eq. (11) is taken, the contribution of the truncated modes to the state response vector can be statically approximated as

$$\Phi_t p_t \approx -\Phi_t \Lambda_t^{-1} \Psi_t^T F = Q_1 F \tag{12}$$

where $Q_1 = -\Phi_t \Lambda_t^{-1} \Psi_t^T$ and will be redefined later in Eq. (17).

Equation (12) is mostly used in previous studies and can be called a first-order approximation of truncated modes. The improvement made in this paper is based on also retaining the first dynamic term in the infinite series, so that the inertia and damping effects of the truncated modes can be taken into account as well. Then the second-order approximation of the truncated modes can be first written as

$$\Phi_t p_t \approx (Q_1 + j\omega Q_2)F = Q_1 F + Q_2 \dot{F} = \Phi_{a1} p_a + \Phi_{a2} \dot{p}_a \tag{13}$$

where $Q_2 = -\Phi_t \Lambda_t^{-2} \Psi_t^T$ and will be redefined later in Eq. (17).

In Eq. (13), the state-space residual attachment modes Φ_{a1} defined as Φ_a in Eq. (8) and the improvement Φ_{a2} are columns of matrices Q_1 and Q_2, respectively, corresponding to the displacement interface DOF and the external excitation DOF in F, and they can be obtained by setting $F = F_a$ in Eq. (13); that is,

$$\Phi_{a1} = Q_1 F_a \qquad \Phi_{a2} = Q_2 F_a \tag{14}$$

where F_a is the state load matrix with load vectors of unit force applied to each displacement interface DOF and external excitation

DOF in F, respectively. The residual attachment mode coordinates p_a will therefore be identical to the displacement interface forces and the external forces in F.

The matrices Q_1 and Q_2 are expressed in terms of the truncated modes in Eqs. (12) and (13); however, for large models, the complete eigensolution is impractical and the truncated modes are often the higher modes for which the eigensolution needs to be obviated. The matrices Q_1 and Q_2 in Eqs. (12) and (13) therefore cannot be used directly and need to be reformulated.

The following identities can be obtained from the biorthogonality of the component modes [i.e., Eq. (10)]:

$$B^{-1} = -\Phi\Lambda^{-1}\Psi^T \tag{15}$$

$$B^{-1}AB^{-1} = \Phi\Lambda^{-2}\Psi^T \tag{16}$$

With the identities in Eqs. (15) and (16), the matrices Q_1 and Q_2 in Eq. (13) can be reformulated as

$$\begin{aligned} Q_i &= -\Phi_t\Lambda_t^{-i}\Psi_t^T \\ &= (-1)^{i-1}B^{-1}(AB^{-1})^{i-1} + \Phi_k\Lambda_k^{-i}\Psi_k^T \qquad i = 1, 2 \end{aligned} \tag{17}$$

where only the eigensolutions of the kept modes are required. The inversion of matrix B is calculated by independent inversion of matrices K and M.

When the improved residual attachment modes (i.e., the second-order approximation of truncated modes) are adopted, the transformation defined by Eq. (8) can be extended as

$$y \approx \begin{pmatrix} \Phi_k & \Phi_{a1} & \Phi_{a2} \end{pmatrix} \begin{pmatrix} p_k \\ p_a \\ \dot{p}_a \end{pmatrix} = \bar{\Phi} p \tag{18}$$

where p_a indicates the residual attachment mode coordinates that are identified with the interface forces and external forces in the state load vector F.

B. Defective Components with Rigid-Body Modes

Assuming that the stiffness matrix K in Eq. (1) is rank-deficient with $\text{rank}(K) = n - n_r$, the component will have a number of n_r displacement rigid-body modes that have eigenvalues of $\lambda_r = 0$ and eigenvectors that satisfy

$$K\varphi_{\text{rd}}^d = 0 \tag{19}$$

For displacement rigid-body eigenvectors φ_{rd}^d, two cases exist in the state space:

1) For case 1, $C\varphi_{\text{rd}}^d = 0$. This implies that the component is completely free and its rigid-body motion does not produce any damping forces; the state rigid-body modes corresponding to a single zero eigenvalue are then

$$\varphi_{\text{rd}} = \begin{pmatrix} \varphi_{\text{rd}}^d \\ 0 \end{pmatrix} \qquad \varphi_{\text{grd}} = \begin{pmatrix} 0 \\ \varphi_{\text{rd}}^d \end{pmatrix} \tag{20}$$

which are called regular and generalized state rigid-body modes, respectively, and they satisfy the following condition:

$$A\begin{pmatrix} \varphi_{\text{rd}} & \varphi_{\text{grd}} \end{pmatrix} \begin{pmatrix} 0 & 1 \\ 0 & 0 \end{pmatrix} + B\begin{pmatrix} \varphi_{\text{rd}} & \varphi_{\text{grd}} \end{pmatrix} = 0 \tag{21}$$

In this case, the eigensystem is defective, as is the component.

2) For case 2, $C\varphi_{\text{rd}}^d \neq 0$. There is then only one regular state rigid-body mode in the state space corresponding to this displacement rigid-body mode. And this type of state rigid-body mode does not produce the defectiveness of the state eigensystem. Thus, the state rigid-body-mode matrix can be expressed as

$$\Phi_r = \begin{pmatrix} \Phi_{\text{rd}}^d & O \\ O & \Phi_{\text{rc}}^d \end{pmatrix} \tag{22}$$

where Φ_{rd}^d denotes all displacement rigid-body eigenvectors φ_{rd}^d, and Φ_{rc}^d denotes the rigid-body eigenvectors satisfying $C\varphi_{\text{rd}}^d = 0$.

In a similar manner, the left state rigid-body modes can be defined as

$$\Psi_r = \begin{pmatrix} \Psi_{\text{rd}}^d & O \\ O & \Psi_{\text{rc}}^d \end{pmatrix} \tag{23}$$

It can be seen from Eq. (21) that the state rigid-body modes are not fully decoupled for defective components; however, it can be shown that the decoupling still exists between state rigid and state elastic modes.

For defective components, Eqs. (13) and (17) cannot be implemented because of the singularity of matrix B; the residual inertia-relief attachment modes were therefore developed to complement the responses of the truncated modes.

C. Brief Review of Residual Inertia-Relief Attachment Modes of Damped Systems

In the free-interface CMS procedure, projection matrices were developed to eliminate the rigid-body components of motion from the total state response and to transform the load vector to a self-equilibrated load of original load and rigid-body inertia forces [11]. For asymmetric systems, they are defined as

$$P^T = I - \Phi_r\bar{A}_{rr}^{-1}\Psi_r^T A \tag{24}$$

and

$$Q = I - A\Phi_r\bar{A}_{rr}^{-1}\Psi_r^T \tag{25}$$

where $\bar{A}_{rr}^{-1}$ is the inverse of rigid-body modal state mass matrix $\Psi_r^T A\Phi_r$.

To approximate the state responses of the truncated modes, with the state stiffness matrix B, which is singular here, the following unusual static problem needs to be solved:

$$B(\Phi_{\text{ek}}p_{\text{ek}} + \Phi_t p_t) = QF \tag{26}$$

where Φ_{ek} and Φ_t denote the kept state elastic modes and the truncated state elastic modes, respectively.

The solution corresponding to the truncated modes is

$$\Phi_t p_t = P^T GQF - \Phi_{\text{ek}}(-\Lambda_{\text{ek}}^{-1})\Psi_{\text{ek}}^T F = (G_e - G_k)F = G_a F \tag{27}$$

where G is the pseudoflexibility matrix of the component. G_e, G_k, and G_a are defined as the flexibility matrix, kept flexibility matrix, and residual flexibility matrix of the component, respectively:

$$G_e = P^T GQ = \Phi_e(-\Lambda_e^{-1})\Psi_e^T \tag{28}$$

$$G_k = \Phi_{\text{ek}}(-\Lambda_{\text{ek}}^{-1})\Psi_{\text{ek}}^T \tag{29}$$

$$G_a = G_e - G_k \tag{30}$$

The residual inertia-relief attachment modes are now obtained as

$$\Phi_a = G_a F_a \tag{31}$$

Then the contribution of the truncated modes to the state response vector is first-order, approximated as

$$\Phi_t p_t \approx \Phi_a p_a = G_a F \tag{32}$$

D. Improved Residual Inertia-Relief Attachment Modes

All dynamic effects of truncated modes are ignored in the approximate expression (32), which is derived from the static equation of motion (26). Contrastively, the exact dynamic equation of motion of defective components can be expressed as

$$B(\Phi_{\mathrm{ek}} p_{\mathrm{ek}} + \Phi_t p_t) = QF - A(\Phi_{\mathrm{ek}} \dot{p}_{\mathrm{ek}} + \Phi_t \dot{p}_t) \tag{33}$$

Substituting the first-order derivative of the solution of Eq. (26) into the right side of Eq. (33) yields

$$B(\Phi_{\mathrm{ek}} p_{\mathrm{ek}} + \Phi_t p_t) = QF - AG_e \dot{F} \tag{34}$$

The solution of Eq. (34) can be confirmed as

$$\Phi_{\mathrm{ek}} p_{\mathrm{ek}} + \Phi_t p_t = P^T GQF - P^T GAG_e \dot{F} \tag{35}$$

According to the definition of the projection matrix Q defined in Eq. (25) and the orthogonality between the state rigid and state elastic modes (i.e., $\Psi_r^T A \Phi_e = 0$), the following projection relation can be obtained:

$$QAG_e = (I - A\Phi_r \bar{A}_{rr}^{-1} \Psi_r^T) A \Phi_e (-\Lambda_e^{-1}) \Psi_e^T = AG_e \tag{36}$$

Substituting the projection Eq. (36) into Eq. (35) for the second term on the right side of Eq. (35), one can obtain the following second-order approximation for the truncated modes:

$$\Phi_t p_t \approx G_a F - G_e AG_e \dot{F} = \Phi_{a1} p_a + \Phi_{a2} \dot{p}_a \tag{37}$$

where the matrix $\Phi_{a1} = G_a F_a$ is the residual inertia-relief attachment mode defined as Φ_a in Eq. (31), and the matrix $\Phi_{a2} = -G_e AG_e F_a$ is the improvement for Φ_{a1}.

The improvement thus made is evident by comparing with the right sides of Eqs. (32) and (37); that is, the dynamic response components of all the elastic modes in terms of $G_e AG_e \dot{F}$ are removed from the static approximation. It is also noted that Eq. (37) has a similarity with Rubin's formulation [5] in the displacement space, but only static contributions of the retained modes are removed from the pseudostatic solution Eq. (35) for obtaining $\Phi_t p_t$ in this paper, rather than the dynamic responses of retained modes, which are also removed in Rubin's approach.

Finally, the transformation similar to Eq. (18) can be written for defective components:

$$y \approx \begin{pmatrix} \Phi_k & \Phi_{a1} & \Phi_{a2} \end{pmatrix} \begin{pmatrix} p_k \\ p_a \\ \dot{p}_a \end{pmatrix} = \bar{\Phi} p \tag{38}$$

E. Relationship Between Residual Attachment Modes of Nondefective and Defective Components

To show the relationship between the residual attachment modes of nondefective and defective components, formulations for the defective components [i.e., Eqs. (24–37)] are applied to nondefective components. In this situation, Φ_r and Ψ_r vanish, and $P = Q = I$ and $G_e = B^{-1}$; thus, G_a and $G_e AG_e$ can be rewritten as

$$G_a = B^{-1} + \Phi_{\mathrm{ek}} \Lambda_{\mathrm{ek}}^{-1} \Psi_{\mathrm{ek}}^T \tag{39}$$

$$G_e AG_e = B^{-1} AB^{-1} \tag{40}$$

The following relationships are obtained for nondefective and defective components by comparing Eq. (17) with Eqs. (39) and (40):

$$Q_1 = G_a \tag{41}$$

$$Q_2 - \Phi_k \Lambda_k^{-2} \Psi_k^T = G_e AG_e \tag{42}$$

Equation (41) implies that the first-order approximations for nondefective and defective components are equivalent; however, Eq. (42) shows that the dynamic term $\Phi_k \Lambda_k^{-2} \Psi_k^T$ is absent in the second-order approximation for defective components, compared with that for nondefective components, which is due to the fact that Eq. (34) is always solved in a pseudostatic sense, but Eq. (17) for $i = 2$ is not solved in this sense.

IV. Mode Selection Criterion

For the establishment of mode selection criterion, Eq. (1) and the displacement response partition of Eq. (7) are first transformed to the frequency domain; respectively, they are

$$X(j\omega) = H(j\omega)\tilde{f}(j\omega) \tag{43}$$

and

$$X(j\omega) = \sum_{i=1}^{2n} \varphi_i P_i(j\omega) \tag{44}$$

where $X(j\omega)$, $\tilde{f}(j\omega)$, and $P_i(j\omega)$ are the Fourier transforms of $x(t)$, $f(t)$, and $p_i(t)$, respectively, and

$$H(j\omega) = (-\omega^2 M + j\omega C + K)^{-1}$$

is the displacement FRF matrix.

Modal responses $P_i(j\omega)$ can be easily determined in the state-modal space in the frequency domain (considering the nondefective case, for example):

$$P_i(j\omega) = \frac{\varphi_i^T \tilde{f}(j\omega)}{j\omega - \lambda_i} \tag{45}$$

The FRF matrix can be expanded in terms of state-modal quantities by substituting Eq. (44) into Eq. (45):

$$H(j\omega) = \sum_{i=1}^{2n} \frac{\varphi_i \varphi_i^T}{j\omega - \lambda_i} \tag{46}$$

In fact, for underdamped modes, each pair of complex conjugate modes represents one vibration mode with the same damping exponent, which is defined as the real part of the complex eigenvalues, and damped eigenfrequency, which is defined as the imaginary part of the complex eigenvalues. Thus, it is convenient to rewrite Eq. (46) as

$$H(j\omega) = \sum_{i=1,3,\ldots,N_1} \left(\frac{\varphi_i \varphi_i^T}{j\omega - \lambda_i} + \frac{\varphi_{i+1} \varphi_{i+1}^T}{j\omega - \lambda_{i+1}} \right) + \sum_{i=1,3,\ldots,N_2} \frac{\varphi_i \varphi_i^T}{j\omega - \lambda_i} \tag{47}$$

where $\lambda_{i+1} = \lambda_i^*$ and $\varphi_{i+1} = \varphi_i^*$ for $i = 1, 3, \ldots, N_1$ are underdamped modes, and λ_i for $i = 1, 3, \ldots, N_2$ are overdamped modes.

It is known from Eq. (46) or Eq. (47) that an error will be introduced to $H(j\omega)$ when the mode truncation is applied to reduce the system size. The error is defined as a norm of difference between $H(j\omega)$ and $\tilde{H}(j\omega)$, approximated by the mode truncation:

$$\begin{aligned} e(j\omega) &= \|H(j\omega) - \tilde{H}(j\omega)\| \\ &= \left\| \sum_{\substack{i=1,3,\ldots,N_1 \\ i \notin R}} \left(\frac{\varphi_i \varphi_i^T}{j\omega - \lambda_i} + \frac{\varphi_{i+1} \varphi_{i+1}^T}{j\omega - \lambda_{i+1}} \right) + \sum_{\substack{i=1,3,\ldots,N_2 \\ i \notin R}} \frac{\varphi_i \varphi_i^T}{j\omega - \lambda_i} \right\| \\ &\le \|\varphi_i\|_{\max}^2 \left[\sum_{\substack{i=1,3,\ldots,N_1 \\ i \notin R}} \left(\frac{1}{|j\omega - \lambda_i|} + \frac{1}{|j\omega - \lambda_{i+1}|} \right) \right. \\ &\quad \left. + \sum_{\substack{i=1,3,\ldots,N_2 \\ i \notin R}} \frac{1}{|j\omega - \lambda_i|} \right] \end{aligned} \tag{48}$$

where R indicates the set of integers as an index of the retained modes.

It is desirable to keep $e(j\omega)$ low when only a small number of modes are retained. This implies that modes that have larger values of S_i^* are important to $H(j\omega)$ if one defines

$$S_i^*(j\omega) = \left(\frac{1}{|j\omega - \lambda_i|} + \frac{1}{|j\omega - \lambda_{i+1}|} \right) \tag{49}$$

or

$$S_i^*(j\omega) = \frac{1}{|j\omega - \lambda_i|} \tag{50}$$

for underdamped and overdamped modes, respectively.

Thus, for the largest damped system eigenfrequency ω_{ds} of interest, a reasonable criterion for the importance of modes can be constructed as

$$S_i = \frac{1}{s\omega_{\mathrm{ds}}} \int_0^{s\omega_{\mathrm{ds}}} S_i^* \, \mathrm{d}\omega \tag{51}$$

where $s > 1$ is a proportion factor yielding the boundary frequency used in the criterion for a component.

The selection of s is usually based on the accuracy and effectiveness of the synthesis approach employed: smaller s applies to more accurate and more effective approaches, and vice versa. The values of 1.5–1.8 are recommended based on the numerical results for the second-order and the first-order approximations, respectively.

This criterion is different from those used in previous works, such as directly retaining a few first pairs of modes or based directly on the absolute values of complex spectra. Instead, it is dependent on the contribution of each pair of underdamped complex modes or overdamped modes to the FRF matrix that characterizes the response of the entire component.

It is also relevant to note that eigenvalues dominate the values of S_i, and thus a complete eigensolution is not necessary for selecting the important modes retained by the criterion.

V. State-Level Synthesis of Damped Components

A standard procedure for the synthesis of damped components is accomplished via applying the following transformation to the dynamic equation of motion of the components in the state-modal space:

$$\begin{pmatrix} p_{\mathrm{indpt}} \\ p_{\mathrm{dpt}} \end{pmatrix} = T p_{\mathrm{indpt}} \tag{52}$$

where p_{indpt} and p_{dpt} denote independent and dependent modal coordinates, and they normally refer to p_k and $(\,p_a^T \quad \dot{p}_a^T\,)^T$, respectively.

The transformation matrix T in Eq. (52) can be identified by constraint conditions on the interfaces between adjacent components, and it plays a significant role in the synthesis procedure.

Consider a system subdivided into two adjacent components named α and β, respectively, for example. Although it is also assumed that there are no external excitations acting on the components, they can be added in a straightforward way in the synthesis procedure.

The most basic constraint conditions are the interface displacement continuity and the interface force equilibrium, which are widely used in previous works for the synthesis of the components:

$$^{\alpha}x_j = {}^{\beta}x_j \tag{53}$$

$$^{\alpha}f_j + {}^{\beta}f_j = 0 \tag{54}$$

where subscript j denotes the interface. It is found, however, that when the improved (second-order approximation) residual attachment modes are employed, the state level of conditions (53) and (54) have to be introduced to transform the dependent set of modal coordinates to the independent set. The state-level conditions are

$$\begin{pmatrix} {}^{\alpha}x_j \\ {}^{\alpha}\dot{x}_j \end{pmatrix} = \begin{pmatrix} {}^{\beta}x_j \\ {}^{\beta}\dot{x}_j \end{pmatrix} \tag{55}$$

$$\begin{pmatrix} {}^{\alpha}p_a \\ {}^{\alpha}\dot{p}_a \end{pmatrix} + \begin{pmatrix} {}^{\beta}p_a \\ {}^{\beta}\dot{p}_a \end{pmatrix} = 0 \tag{56}$$

where the fact that the residual attachment modal coordinates p_a are equivalent to the interface forces f_j is recognized [13].

Equation (55) implies that

$$\begin{aligned} &{}^{\alpha}\Phi_{kj}\,{}^{\alpha}p_k + {}^{\alpha}\Phi_{a1j}\,{}^{\alpha}p_a + {}^{\alpha}\Phi_{a2j}\,{}^{\alpha}\dot{p}_a \\ &\quad = {}^{\beta}\Phi_{kj}\,{}^{\beta}p_k + {}^{\beta}\Phi_{a1j}\,{}^{\beta}p_a + {}^{\beta}\Phi_{a2j}\,{}^{\beta}\dot{p}_a \end{aligned} \tag{57}$$

Substituting Eq. (56) into Eq. (57), one obtains

$$\begin{pmatrix} {}^{\alpha}\Phi_{a1j} + {}^{\beta}\Phi_{a1j} & {}^{\alpha}\Phi_{a2j} + {}^{\beta}\Phi_{a2j} \end{pmatrix} \begin{pmatrix} {}^{\alpha}p_a \\ {}^{\alpha}\dot{p}_a \end{pmatrix} = \begin{pmatrix} -{}^{\alpha}\Phi_{kj} & {}^{\beta}\Phi_{kj} \end{pmatrix} \begin{pmatrix} {}^{\alpha}p_k \\ {}^{\beta}p_k \end{pmatrix} \tag{58}$$

Thus, the transformation equation (52) for the state-level synthesis can be found as

$$\begin{pmatrix} {}^{\alpha}p_k \\ {}^{\alpha}p_{\mathrm{dpt}} \\ {}^{\beta}p_k \\ {}^{\beta}p_{\mathrm{dpt}} \end{pmatrix} = \begin{pmatrix} {}^{\alpha}I_k & 0 \\ D_1 & D_2 \\ 0 & {}^{\beta}I_k \\ -D_1 & -D_2 \end{pmatrix} \begin{pmatrix} {}^{\alpha}p_k \\ {}^{\beta}p_k \end{pmatrix} \tag{59}$$

where $D_1 = -W\,{}^{\alpha}\Phi_{kj}$ and $D_2 = W\,{}^{\beta}\Phi_{kj}$ with

$$W = \begin{pmatrix} {}^{\alpha}\Phi_{a1j} + {}^{\beta}\Phi_{a1j} & {}^{\alpha}\Phi_{a2j} + {}^{\beta}\Phi_{a2j} \end{pmatrix}^{-1}$$

With this transformation, the synthesized (reduced) system can then be obtained as

$$A_s \dot{p}_{\mathrm{indpt}} + B_s p_{\mathrm{indpt}} = F_s \tag{60}$$

where

$$A_s = T^T \begin{pmatrix} {}^{\alpha}\bar{A} & 0 \\ 0 & {}^{\beta}\bar{A} \end{pmatrix} T$$

$$B_s = T^T \begin{pmatrix} {}^{\alpha}\bar{B} & 0 \\ 0 & {}^{\beta}\bar{B} \end{pmatrix} T$$

$$F_s = T^T \begin{pmatrix} {}^{\alpha}\bar{F} \\ {}^{\beta}\bar{F} \end{pmatrix}$$

$$p_{\mathrm{indpt}} = \begin{pmatrix} {}^{\alpha}p_k \\ {}^{\beta}p_k \end{pmatrix}$$

with $\bar{A} = \bar{\Phi}^T A \bar{\Phi}$, $\bar{B} = \bar{\Phi}^T B \bar{\Phi}$, and $\bar{F} = \bar{\Phi}^T F$ (if only interface forces exist, F_s will vanish).

VI. Summary of the Method

An improved component-mode-synthesis method for nonclassically damped systems was developed, and the method can be summarized as follows:

1) For a given nonclassically damped dynamic system, partition it into several smaller components represented by Eq. (1). Then transform Eq. (1) into state-space form [i.e., Eq. (2)] by using Eqs. (3) and (4).

2) Solve the generalized complex eigenproblem Eq. (5) and the adjoint eigenproblem Eq. (6) and normalize the eigenvectors according to Eq. (10). Note that the complete eigensolution is not necessary.

3) For each elastic mode solved in step 2, calculate S_i defined in Eq. (51) to rank the importance of each mode.

4) Based on the feature of S_i of the modes, select modes with at least a ratio of $S_i/[S_i]_{\max}$ larger than 50% as retained modes. A smaller value of the ratio then used more retained modes and greater accuracy was achieved.

5) With the retained elastic modes, calculate matrices Q_1 and Q_2 by using Eq. (17) for nondefective components or calculate matrices G_a and $-G_eAG_e$ by using Eqs. (28–30) for defective components.

6) Extract columns from Q_1 and Q_2 for nondefective components or from G_a and $-G_eAG_e$ for defective components corresponding to displacement interface DOF and external excitation DOF in F to obtain modal matrices Φ_{a1} and Φ_{a2}.

7) For defective components, verify whether the displacement rigid-body modes satisfy $C\varphi^d_{\text{rd}} = 0$ and construct state rigid-body modes according to Eq. (20) or Eq. (22). Retain all state rigid-body modes for defective components together with the elastic modes retained in step 4.

8) Obtain modal transformation matrix Eq. (18) or Eq. (38) for nondefective and defective components, respectively. Transform each component into state-modal space with transformations $\bar{A} = \bar{\Phi}^T A \bar{\Phi}$, $\bar{B} = \bar{\Phi}^T B \bar{\Phi}$, and $\bar{F} = \bar{\Phi}^T F$.

9) Calculate transformation matrix T defined in Eq. (52) by using Eq. (59).

10) The synthesized system is Eq. (60) with transformations

$$A_s = T^T \begin{pmatrix} {}^{\alpha}\bar{A} & 0 \\ 0 & {}^{\beta}\bar{A} \end{pmatrix} T$$

$$B_s = T^T \begin{pmatrix} {}^{\alpha}\bar{B} & 0 \\ 0 & {}^{\beta}\bar{B} \end{pmatrix} T$$

and

$$F_s = T^T \begin{pmatrix} {}^{\alpha}\bar{F} \\ {}^{\beta}\bar{F} \end{pmatrix}$$

for example, the system is partitioned into two components.

VII. Numerical Application

A. Damped Free–Free Beam Model

To compare the accuracy and effectiveness of the first- and the second-order approximations, a free–free two-dimensional uniform beam, shown in Fig. 1, is selected as the first test model. The beam is made of aluminum with a length of 1.8 m, cross-sectional area of 5.0E-5 m^2, and moments of inertia of 4.17E-10 m^4 and 1.04E-1 m^4, respectively. The beam model is discretized evenly with 20 elements and is divided into two components, α and β. The damping is assumed to be proportional to the stiffness at the element level (i.e., $C_e = 0.0002K_e$ for elements 1 to 5 and 13 to 16, $C_e = 0.0004K_e$ for elements 6 to 12, and $C_e = 0.0001K_e$ for elements 17 to 20, as shown in Fig. 1), but nonclassical at both the component and system levels.

It is assumed that the eigenfrequencies of the system lower than 2000 rad/s are of interest. The proportion factor is selected as $s = 1.5$, and the importance of each mode ranked by Eq. (51) is described in Fig. 2 for those modes lower than 3000 rad/s. In Fig. 2 , for component α, the first 5 S_i correspond to the first 5 conjugated mode pairs and the last 3 S_i correspond to the next 3 overdamped modes; for component β, the first 4 S_i correspond to the first 4 conjugated mode pairs and the last 3 S_i correspond to the next 3 overdamped modes. It is seen that the S_i starts to level off at $n = 6$ and 5 for components α and β, respectively, with a reduction of S_i larger than 90%, where n is the number of underdamped conjugated mode pairs or overdamped modes. Therefore, the first 11 and 9 complex elastic modes (including overdamped modes) are kept, based on this feature, with the criterion for components α and β, respectively, in this case. The DOF of the components and their kept modes for the synthesis are summarized in Table 1. Table 2 lists the damping exponents σ and damped eigenfrequencies ω_d of the system, and the slashes for the 11th and 13th damped eigenfrequencies indicate that these modes are overdamped. Comparisons of errors of damping exponents, damped eigenfrequencies, and mode shapes in the state space (mode shape, for brevity, in the following part of this section) obtained, respectively, with the first- and the second-order approximations are presented in Table 3.

As can be seen from Table 3, with the second-order approximation, excellent results (except for the mode shape of the 11th overdamped mode) are obtained for the first 12 modes, among which, the 12th mode is the highest mode of interest. Comparing with the results of the first-order approximation, the enhancement of the accuracy is significant. Here, the mode-shape error is calculated by subtracting the modal assurance criterion (MAC) value from 100%:

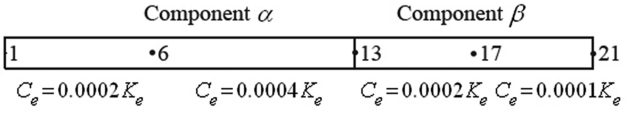

Fig. 1 Free–free beam and defined components.

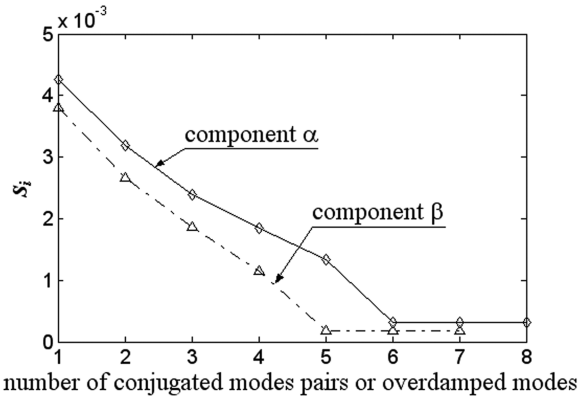

Fig. 2 Modal importance S_i vs the number of conjugated mode pairs or overdamped modes.

Table 2 Eigenvalues of the beam model[a]

Mode order	Damping exponents σ	Damped eigenfrequencies ω_d
3	−0.4337	50.7477
4	−2.5988	139.8767
5	−9.5702	274.1607
6	−24.6380	453.1559
7	−57.2182	675.7058
8	−115.4958	943.3733
9	−193.3861	1253.3579
10	−331.2661	1601.7126
11	−2508.8743	——
12	−505.4707	2007.2358
13	−2512.8477	——
14	−764.2019	2397.0209
15	−1099.8903	2903.9789

[a]Only one of a pair of conjugated complex modes are listed; rigid-body modes are not included.

Table 1 List of the components' DOF and modes for the synthesis of beam model

		First- and second-order approximations		
Components	State DOF	Rigid-body modes	Kept elastic modes	Residual inertia-relief modes
α	26 × 2	4	11	2
β	18 × 2	4	9	2

Table 3 Errors of the first- and the second-order approximations for the beam model[a]

	First-order approximation			Second-order approximation		
Mode order	σ error, %	ω_d error .%	State mode shape error, %	σ error, %	ω_d error, %	State mode shape error, %
3	0.0013	0.0005	0.1549	0.0000	0.0000	0.0000
4	0.0006	0.0015	0.1926	0.0000	0.0000	0.0000
5	0.0182	0.0055	0.4047	0.0000	0.0000	0.0000
6	0.0304	0.0343	1.6766	0.0000	0.0006	0.0007
7	0.0675	0.0107	0.0939	0.0013	0.0001	0.0001
8	0.3540	0.2055	5.3334	0.0223	0.0147	0.0037
9	0.0667	0.0790	0.2244	0.0442	0.0075	0.0010
10	2.1039	0.7141	10.560	0.4101	0.1381	0.1005
11	2.0332	——	93.601	4.1836	——	79.828
12	3.5818	0.6295	2.1508	1.7928	0.2114	0.2209
13		missing			missing	
14	2.9543	12.872	66.574	1.8059	6.3489	15.861
15	176.42	48.913	81.456	18.991	16.398	44.560

[a]Errors of only one of a pair of conjugated complex modes are listed; rigid-body modes are not included.

$$\mathrm{MAC}\,(\varphi_{\mathrm{exact}}, \varphi_{\mathrm{app}}) = \frac{(\varphi_{\mathrm{exact}}^T \varphi_{\mathrm{app}})^2}{(\varphi_{\mathrm{exact}}^T \varphi_{\mathrm{exact}})(\varphi_{\mathrm{app}}^T \varphi_{\mathrm{app}})}$$

For comparison purposes, Figs. 3–8 show the numbers and mean errors of the damping exponents, eigenfrequencies, and mode shapes with errors less than 0.1% as a function of the numbers of the final synthesized DOF for first- and second- order approximations. The overall effectiveness and accuracy of the second-order approximation over the first can be observed from Figs. 3–8. As shown in Figs. 5 and 8, the accuracy of the mode shapes calculated with the second-order approximation is even more remarkable than those with the first-order approximation. There are no mode shapes with errors less than 0.1% for first-order approximation when the number of the final synthesized DOF is less than 30, but the same is not true for second-order approximation. The fact that the mean errors shown in Figs. 6–8 do not always decrease with the number of the final synthesized DOF is because increased numbers of damping exponents, eigenfrequencies, or mode shapes are used to calculate the mean errors for increased numbers of final synthesized DOF.

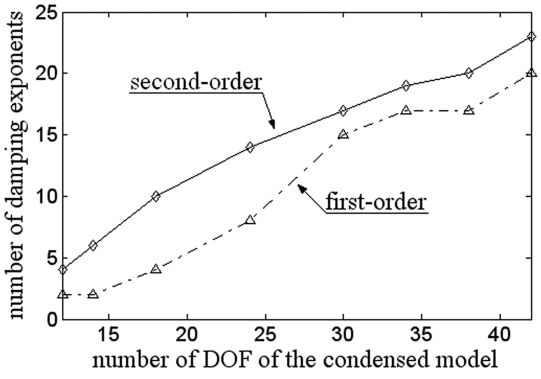

Fig. 3 Number of damping exponents of elastic modes with errors less than 0.1% vs the number of DOF of the condensed model.

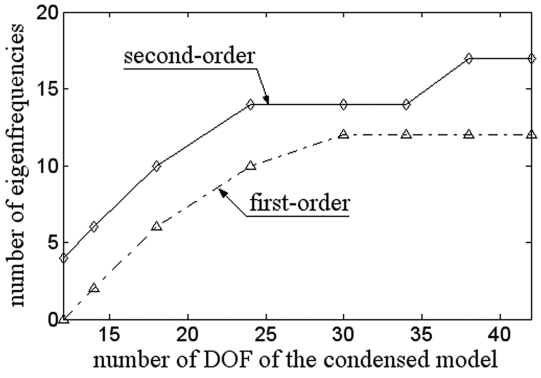

Fig. 4 Number of eigenfrequencies of elastic modes with errors less than 0.1% vs the number of DOF of the condensed model.

B. Damped Satellite Structure

The second application presented here is a complex satellite structure, which is mainly made of composite material and equipped with constrained viscoelastic damping layers for vibration attenuation during launch. The structure is modeled with a finite element model of 45,504 DOF and is divided into two components according to the requirements of the launch vehicle and spacecraft departments, as shown in Fig. 9. The model is ground-fixed in the

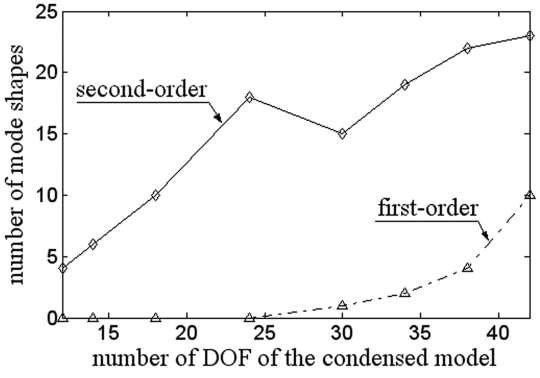

Fig. 5 Number of elastic mode shapes with errors less than 0.1% vs the number of DOF of the condensed model.

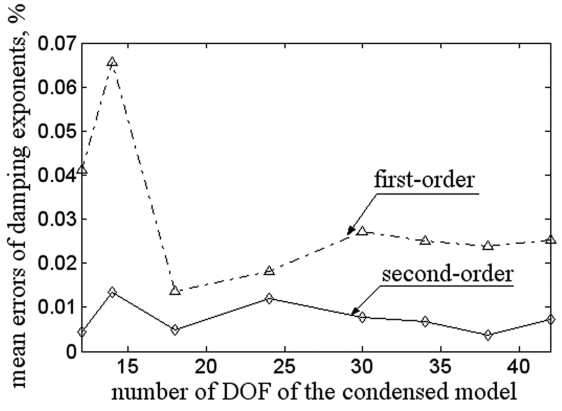

Fig. 6 Mean errors of damping exponents of elastic modes with errors less than 0.1% vs the number of DOF of the condensed model.

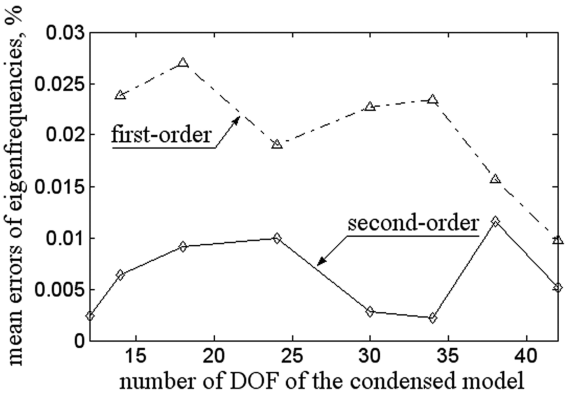

Fig. 7 Mean errors of eigenfrequencies of elastic modes with errors less than 0.1% vs the number of DOF of the condensed model.

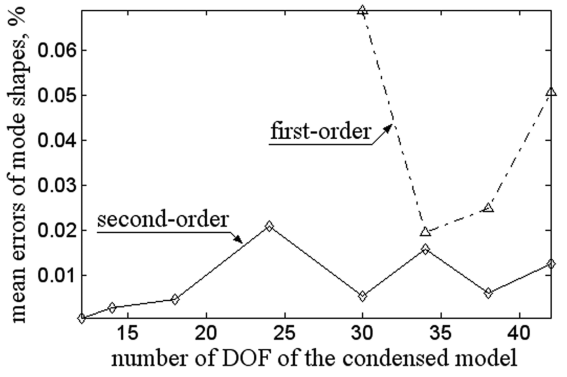

Fig. 8 Mean errors of elastic mode shapes with errors less than 0.1% vs the number of DOF of the condensed model.

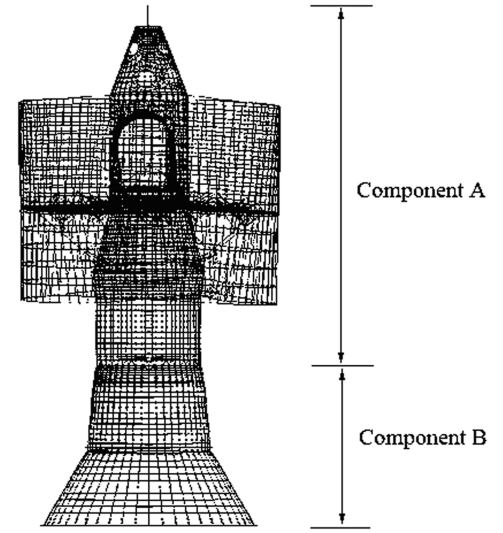

Fig. 9 Finite element model of the satellite structure (with a certain mode shape).

modal analysis to simulate the boundary condition of the satellite during launch, then component A is defective and component B is nondefective.

The modes of the structure lower than 250 rad/s (corresponding to the first 20 modes) are of interest. The proportional factor $s = 1.5$ is adopted here again. Modal importance ranking for the first 15 pairs of conjugated modes of components A and B is shown in Figs. 10 and 11, respectively. It is seen from Fig. 10 that the reduction of S_i is larger than 60% after the first 11 pairs of conjugated modes for

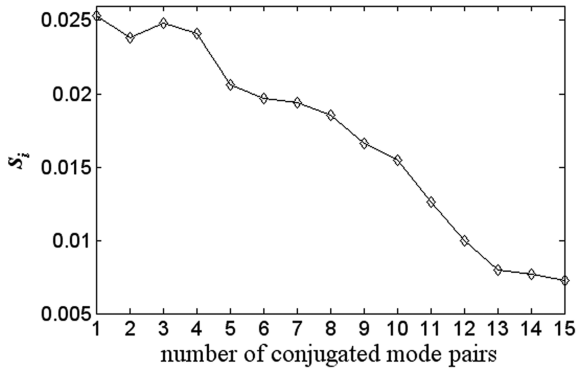

Fig. 10 Modal importance S_i of component A vs the number of conjugated mode pairs.

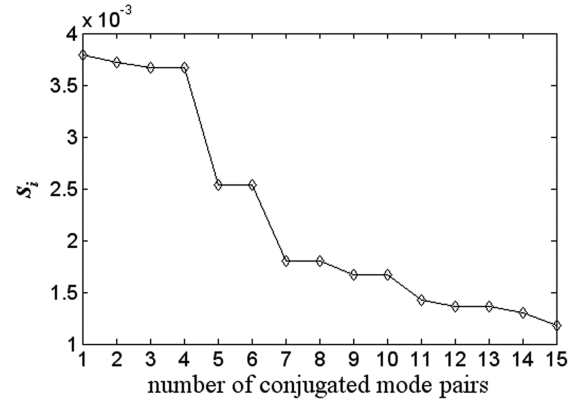

Fig. 11 Modal importance S_i of component B vs the number of conjugated mode pairs.

component A, and thus the first 11 pairs of conjugated modes are kept for component A. For component B, it is seen from Fig. 11 that the first 4 pairs of conjugated modes possess nearly the same largest S_i and the S_i of the higher modes rapidly reduce to a low neglectable level; therefore, only the first 4 pairs of conjugated modes are retained, although the fifth and sixth pairs of conjugated modes also appear to be retainable. The thus-synthesized model has an order of 42 after adding the 12 state rigid-body modes of component A.

Damping exponents and damped eigenfrequencies of the satellite structure are listed in Table 4. Errors of the damping exponents and damped eigenfrequencies calculated with the first- and second-order approximations, respectively, are presented in Table 5. It is observed that good accuracies are achieved for the damped eigenfrequencies, especially those obtained by the second-order approximation, but errors of the damping exponents are relatively large for both first- and second-order approximations. This implies that the synthesis procedure may not simultaneously give the same accuracy to damping exponents and damped eigenfrequencies. However, an

Table 4 Eigenvalues of the satellite structure[a]

Mode order	Damping exponents σ	Damped eigenfrequencies ω_d
1	−0.8395	68.4193
2	−0.8469	68.7640
3	−2.9886	129.0115
4	−7.0029	201.7632
5	−7.2361	205.5765
6	−9.0252	252.2607
7	−9.5487	232.8923
8	−11.1379	235.3817
9	−11.1276	244.7533
10	−12.8737	251.7269

[a]Only one of a pair of conjugated complex modes are listed.

Table 5 Errors of the first- and the second-order approximations for the satellite structure[a]

	First-order approximation		Second-order approximation	
Mode order	σ error, %	ω_d error, %	σ error, %	ω_d error, %
1	8.5470	0.0264	8.4834	0.0018
2	8.3442	0.0278	8.2776	0.0018
3	6.7385	0.4570	7.7128	0.0061
4	3.2784	0.5004	2.2822	0.0353
5	1.6105	0.5894	0.1381	0.0354
6	4.5608	0.7170	2.2995	0.0542
7	3.1873	0.6188	2.1722	0.1110
8	22.942	0.3172	23.472	0.0478
9	10.751	1.0351	8.9272	0.0678
10	19.180	1.0420	23.264	0.1005

[a]Errors of only one of a pair of conjugated complex modes are listed.

overall better accuracy can also be seen for the second-order approximation.

VIII. Conclusions

An improved component-mode-synthesis method for nonclassically damped systems is developed. Static flexibility and dynamic effects of truncated complex modes are both taken into account by the second-order approximations. As a result of adding the second-order terms, the size of the reduced model in the component level is increased; nevertheless, in the state-level synthesis, the order of the reduced system is exactly the same as when they are not used.

The criterion for the selection of retained complex modes is established on the frequency average of the FRF errors. With this criterion, a complete eigensolution is generally not required to determine the retained modes, although the proportional factor s needs to be determined by some further studies.

The numerical results indicate that the improved synthesis procedure can lead to greater model accuracy and more effective model reduction than can be achieved by the static approximation. However, caution should be taken when the synthesis procedure is applied to a complicated and large structure, because the second-order approximation may not provide a sufficiently high accuracy for the calculated damping exponents.

References

[1] Hurty, W. C., "Dynamic Analysis of Structural Systems Using Component Modes," *AIAA Journal*, Vol. 3, No. 4, 1965, pp. 678–685.

[2] Craig, R. R., and Bampton, M. C. C., "Coupling of Substructures for Dynamic Analyses," *AIAA Journal*, Vol. 6, No. 7, 1968, pp. 1313–1319.

[3] MacNeal, R. H., "Hybrid Method of the Component Mode Synthesis," *Computers and Structures*, Vol. 1, No. 4, 1971, pp. 581–601. doi:10.1016/0045-7949(71)90031-9

[4] Hintz, R. M., "Analytical Methods in Component Modal Synthesis," *AIAA Journal*, Vol. 13, No. 8, 1975, pp. 1007–1016.

[5] Rubin, S., "Improved Component-Mode Representation for Structural Dynamic Analysis," *AIAA Journal*, Vol. 13, No. 8, 1975, pp. 995–1006.

[6] Craig, R. R., and Chang, C. J., "Free-Interface Methods of Substructure Coupling for Dynamic Analysis," *AIAA Journal*, Vol. 14, No. 11, 1976, pp. 1633–1635.

[7] Suarez, L. E., and Singh, M. P., "Improved Fixed Interface Method for Modal Synthesis," *AIAA Journal*, Vol. 30, No. 12, 1992, pp. 2952–2958.

[8] Kang, J. H., and Kim, Y. Y., "Field-Consistent Higher-Order Free-Interface Component Mode Synthesis," *International Journal for Numerical Methods in Engineering*, Vol. 50, No. 3, 2001, pp. 595–610. doi:10.1002/1097-0207(20010130)50:3<595::AID-NME39>3.0.-CO;2-5

[9] Howsman, T. G., and Craig, R. R., "A Substructure Coupling Procedure Applicable to General Linear Time-Invariant Dynamic Systems," *Proceedings of the AIAA/ASME/ASCE 25th Structures, Structural Dynamics, and Materials Conference*, AIAA, New York1984, pp. 164–171.

[10] Beliveau, J. G., and Soucy, Y., "Damping Synthesis Using Complex Substructure Modes and a Hermitian System Representation," *AIAA Journal*, Vol. 23, No. 12, 1985, pp. 1952–1956.

[11] Craig, R. R., and Ni, Z., "Component Mode Synthesis for Model Order Reduction of Nonclassically Damped Systems," *Journal of Guidance, Control, and Dynamics*, Vol. 12, No. 4, 1989, pp. 577–584.

[12] Wang, W., and Kirkhope, J., "Complex Component Mode Synthesis for Damped Systems," *Journal of Sound and Vibration*, Vol. 181, No. 5, 1995, pp. 781–800. doi:10.1006/jsvi.1995.0171

[13] Muravyov, A., and Hutton, S. G., "Component Mode Synthesis for Nonclassically Damped Systems," *AIAA Journal*, Vol. 34, No. 8, 1996, pp. 1664–1669.

[14] Xiang, J., Ren, G., and Lu, Q., "Synthesis Technique for the Nonclassically Damped Structures Using Real Schur Vectors," *AIAA Journal*, Vol. 37, No. 5, 1999, pp. 660–662.

[15] Morgan, J. A., Pierre, C., and Hulbert, G. M., "Baseband Methods of the Component Mode Synthesis for Non-Proportionally Damped Systems," *Mechanical Systems and Signal Processing*, Vol. 17, No. 3, 2003, pp. 589–598.

[16] Craig, R. R. Jr., and Chung, Y. T., "Generalized Substructure Coupling Procedure for Damped Systems," *AIAA Journal*, Vol. 20, No. 3, 1982, pp. 442–444.

[17] Leung, A. Y. T., "Damped Dynamic Substructures," *International Journal for Numerical Methods in Engineering*, Vol. 26, No. 11, 1988, pp. 2355–2365. doi:10.1002/nme.1620261102

[18] Wang, W., and Kirkhope, J., "Component Mode Synthesis for Damped Rotor Systems with Hybrid Interfaces," *Journal of Sound and Vibration*, Vol. 177, No. 3, 1994, pp. 393–410. doi:10.1006/jsvi.1994.1442

[19] de Kraker, A., and van Campen, D. H., "Rubin's CMS Reduction Method for General State-Space Models," *Computers and Structures*, Vol. 58, No. 3, 1996, pp. 597–606. doi:10.1016/0045-7949(95)00151-6

[20] Garvey, S. D., Friswell, M. I., and Penny, J. E., "Efficient Component Mode Synthesis with Non-Classically Damped (Sub-)Structures," *1998 International Modal Analysis Conference Proceedings (IMAC XVI-98)*, Pt. 2, Society for Experimental Mechanics, Bethel, CT, 1998, p. 1602.

[21] Morgan, J. A., Pierre, C., and Hulbert, G. M., "Component Mode Synthesis Methods for Non-Proportionally Damped Systems," *1999 IMAC Proceedings (IMAC XVII-99)*, Society for Experimental Mechanics, Bethel, CT, 1999, pp. 1472–1480.

[22] Morgan, J. A., and Craig, R. R. Jr., "Comparison of Three Component Mode Synthesis Methods for Non-Proportionally Damped Systems," *41st AIAA/ASME/ASCE/AHS/ASC Structures, Structural Dynamics, and Materials Conference*, AIAA, Reston, VA, 2000, pp. 211–219.

M. Ahmadian
Associate Editor